Research Journal of Applied Sciences, Engineering and Technology 7(13): 2756-2761, 2014
DOI:10.19026/rjaset.7.597
ISSN: 2040-7459; e-ISSN: 2040-7467

Submitted: September 24, 2013 Accepted: October 23, 2013 Published: April 05, 2014

Research Article

A Double-ended Fault Location Algorithm without Being Affected by Line Parameters

[1, 2]Fanrong Wang and [2]Hong Zhou
[1]School of Electrical and Electronic Engineering, Hubei University of Technology, Wuhan 430068, China
[2]Department of Automation, Wuhan University, Wuhan 430072, China

Abstract: This study presents a ranging algorithm which requires only voltages and currents measured from the two terminals to establish ranging equations. It divides the line into a certain parts and uses every point as failure point to solve three groups of line impedances. When the function which is established by impedance data reaches the minimum, the corresponding point is right the failure point. Simulations show that it can be used for any type of failure and it may not cause ranging error for incorrect parameters.

Keywords: Fault location, line parameters, ranging function, transmission line

INTRODUCTION

High-voltage transmission lines are the lifeblood of the power system, which bears transmit electrical energy. Meanwhile, it has a fault occurs in the power system in most places and is extremely difficult to find. Therefore, in line fault quickly and accurately find the point of failure, not only for timely repair lines and ensure reliable power supply and the power system security, stability and economic operation has a very important role. For a long time, people are seeking effective and accurate fault location method for a lot of research, a variety of fault location principles and methods are proposed. With the development of new technologies, fault location algorithm deepening abroad has become one of the hot spots.

According to signal characteristics, fault location method can be divided into frequency-based fault location and traveling wave fault location. Taking into account the economy, this paper study only frequency-based fault location. Many documents make further research and put forward the improvement method. Guo *et al*. (2003), Qi *et al*. (2005), Huang *et al*. (2009), Huang and Sun (2003) and Yu and Gu (2001) propose some improved algorithms of filtering decaying DC component based on Fourier algorithm. Liang *et al*. (2004) adopts distributed parameter model and it presents a fault location algorithm based on line parameter estimation and calculates the parameters of line ends, eliminating the line parameters and non synchronous angle difference influence on ranging precision. Document (Suonan *et al*., 2006) presents a double-ended fault location algorithm based on parameter identification in the time domain and it overcomes the traditional fault location method for measuring error of line parameters caused by the inaccurate.

Existing fault location algorithms are assuming that distribution transmission line is uniform and line parameters are known. So the exact line parameters directly determine the final degree of error ranging. In practical engineering, Lines tend to be unevenly distributed. Due to reasons such as geographic incomplete rearrangement, parameters are affected by the weather, the line height, etc. Given circuit parameters are often unreliable and the ranging accuracy is very low. To solve this problem, this study focuses on how to improve the basic algorithm of fault location and on this basis, the use of simulation experiments verify the accuracy of fault location methods and practicality. It presents a double-ended fault location algorithm without being affected by line parameters, the principle of the method is to use the idea of constructing a new match ranging function, this algorithm requires only two-terminal voltage measured by the amount of current that can be used Any type of failure, will not lead to inaccurate line parameters ranging error.

METHODOLOGY

Fundamentals:

Single-phase ground fault algorithm principle: Single-phase ground fault is shown in Fig. 1.

$\dot{U}_{MA}$, $\dot{U}_{MB}$, $\dot{U}_{MC}$, are the measured voltages of M side, respectively, $\dot{U}_{NA}$, $\dot{U}_{NB}$, $\dot{U}_{NC}$, are the measured voltages of N side respectively, $\dot{I}_{MA}$, $\dot{I}_{MB}$, $\dot{I}_{MC}$, are the measured output currents of M side, $\dot{I}_{NA}$, is the measured current of N side, the fault distance l is accounted for all the length of percentage.

Corresponding Author: Hong Zhou, Department of Automation, Wuhan University, Wuhan 430072, China

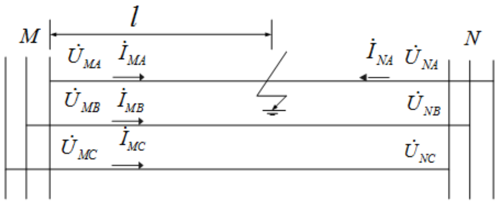

Fig. 1: A phase earth fault schematic diagram

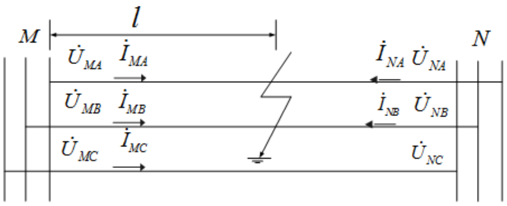

Fig. 2: AB phase earth fault schematic diagram

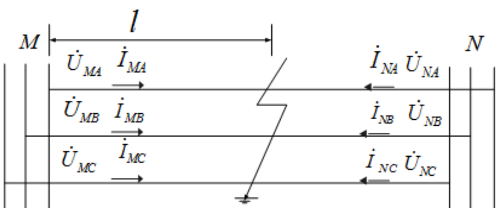

Fig. 3: Three-phase earth fault schematic diagram

By the non-fault phase B, C, equations can be obtained. Where Z_s is self-impedance and Z_M is coupling impedance line:

$$\dot{U}_{MB} - \dot{U}_{NB} = Z_S \dot{I}_{MB} + Z_M \dot{I}_{MC} + lZ_M \dot{I}_{MA} - (1-l) Z_M \dot{I}_{NA} \quad (1)$$

$$\dot{U}_{MC} - \dot{U}_{NC} = Z_S \dot{I}_{MC} + Z_M \dot{I}_{MB} + lZ_M \dot{I}_{MA} - (1-l) Z_M \dot{I}_{NA} \quad (2)$$

Equation (3) and (4) can be obtained by the fault phase A. Where R is the line to ground fault resistance:

$$\dot{U}_{MA} = lZ_S \dot{I}_{MA} + lZ_M (\dot{I}_{MB} + \dot{I}_{MC}) + R(\dot{I}_{MA} + \dot{I}_{NA}) \quad (3)$$

$$\dot{U}_{NA} = (1-l) Z_S \dot{I}_{NA} - (1-l) Z_M (\dot{I}_{MB} + \dot{I}_{MC}) + R(\dot{I}_{MA} + \dot{I}_{NA}) \quad (4)$$

In order to eliminate transition resistance Eq. (5) is obtained by Eq. (3) and (4):

$$\dot{U}_{MA} - \dot{U}_{NA} = lZ_S \dot{I}_{MA} + lZ_M (\dot{I}_{MB} + \dot{I}_{MC}) - (1-l) Z_S \dot{I}_{NA} + (1-l) Z_M (\dot{I}_{MB} + \dot{I}_{MC}) \quad (5)$$

Z_s, Z_M, l are the unknown parameters, which can be solved by Eq. (1), (2) and (5).

Principle of two-phase ground fault and phase fault algorithm: Two-phase ground fault is similar to phase fault. It provides AB phase ground failure as an example for analysis, as shown in Fig. 2.
Equation (6) can be obtained by non-fault phase C:

$$\dot{U}_{MC} - \dot{U}_{NC} = Z_S \dot{I}_{MC} + lZ_M (\dot{I}_{MB} + \dot{I}_{MA}) - (1-l) Z_M (\dot{I}_{NA} + \dot{I}_{NB}) \quad (6)$$

Equation (7) and (8) can be obtained by the fault phase A:

$$\dot{U}_{MA} = lZ_S \dot{I}_{MA} + lZ_M (\dot{I}_{MB} + \dot{I}_{MC}) + \dot{U}_{FA} \quad (7)$$

$$\dot{U}_{NA} = (1-l) Z_S \dot{I}_{NA} + (1-l) Z_M (\dot{I}_{NB} - \dot{I}_{MC}) + \dot{U}_{FA} \quad (8)$$

In Eq. (7) and (8) $\dot{U}_{FA}$ is fault point voltage for the A phase to ground. In order to eliminate $\dot{U}_{FA}$ Eq. (9) is obtained by Eq. (7) and (8):

$$\dot{U}_{MA} - \dot{U}_{NA} = lZ_S \dot{I}_{MA} + lZ_M (\dot{I}_{MB} + \dot{I}_{MC}) - (1-l) Z_S \dot{I}_{NA} - (1-l) Z_M (\dot{I}_{NB} - \dot{I}_{MC}) \quad (9)$$

Equation (10) and (11) can be obtained by fault phase B:

$$\dot{U}_{MB} = lZ_S \dot{I}_{MB} + lZ_M (\dot{I}_{MA} + \dot{I}_{MC}) + \dot{U}_{FB} \quad (10)$$

$$\dot{U}_{NB} = (1-l) Z_S \dot{I}_{NB} + (1-l) Z_M (\dot{I}_{NA} - \dot{I}_{MC}) + \dot{U}_{FB} \quad (11)$$

In Eq. (10) and (11), $\dot{U}_{FB}$ is fault point voltage for the B phase to ground. In order to eliminate $\dot{U}_{FB}$ Eq. (12) is obtained by Eq. (10) and (11):

$$\dot{U}_{MB} - \dot{U}_{NB} = lZ_S \dot{I}_{MB} + lZ_M (\dot{I}_{MA} + \dot{I}_{MC}) - (1-l) Z_S \dot{I}_{NB} - (1-l) Z_M (\dot{I}_{NA} - \dot{I}_{MC}) \quad (12)$$

Z_s, Z_M, l can be solved by Eq. (6), (9) and (12).

Three-phase fault algorithm principle: When three-phase short circuit failure occurs as Fig. 3 shows, the system remains symmetrical, Eq. (12) and (14) can be obtained from the A phase:

$$\dot{U}_{MA} = lZ_1 \dot{I}_{MA} + \dot{U}_{FA} \quad (13)$$

$$\dot{U}_{NA} = (1-l) Z_1 \dot{I}_{NA} + \dot{U}_{FA} \quad (14)$$

In formula (13) and (14) Z_1 is the positive sequence impedance for the whole line. Its value can be calculated in advance across the electrical quantity before the failure:

$$Z_1 = \frac{\dot{U}_{MA}^{pre} - \dot{U}_{MB}^{pre}}{\dot{I}_{MA}^{pre}} \quad (15)$$

Superscript pre is representative of the pre-fault electrical quantities. Equation (16) can be obtained by Eq. (13) minus and (14). l can be solved by Eq. (16):

$$\dot{U}_{MA} - \dot{U}_{NA} = lZ_1 \dot{I}_{MA} - (1-l) Z_1 \dot{I}_{NA} \quad (16)$$

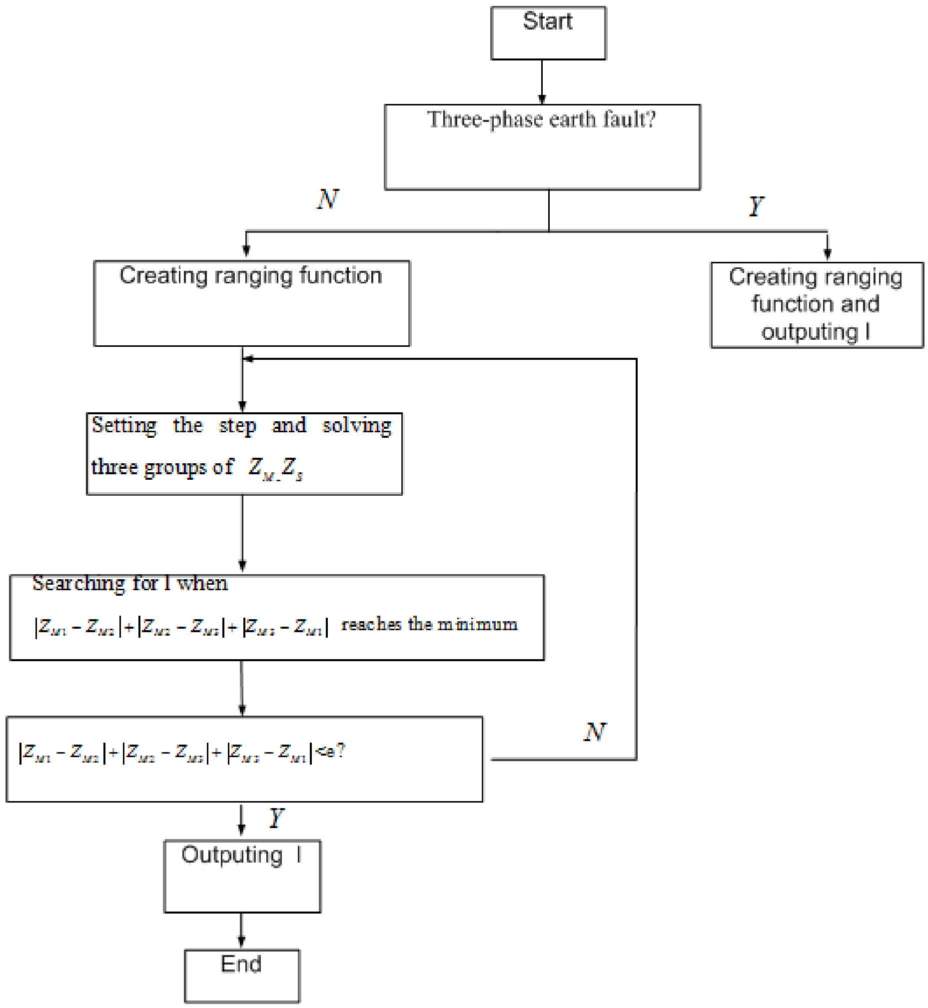

Fig. 4: Program flow diagram

Algorithm realization: Ranging equations derived from earlier are composed of three nonlinear equations except three-phase earth fault. It is hard to directly solve the fault distance and usually pseudo roots appear. This study uses the search method for solving equations. Assuming that the *l*, s initial value, selecting two of the three equations, plugging in *l*, Z_s and Z_M can be easily calculated. Since there are three selection methods, then the solved Z_s, Z_M are three groups, if the value *l* is correct, then the three groups are the same.

In the double-end unsynchronized case, repeating the search can reduce errors. Selecting the appropriate search step between 0 and 1, calculating Z_s, Z_M. It finds the appropriate point in which three groups of calculating value difference is minimum. If the result does not meet the requirement, it may reselect the step size until it gets the optimal solution. By this way, it can find the most appropriate point to Cause error of the three groups of Z_s and Z_M to be smallest. Figure 4 shows the flow chart.

Fig. 5: System simulation model

ALGORITHM SIMULATION

In order to verify the correctness of the algorithm, this study adopts double-ended power supplying about 500 kV EHV transmission line parameters and it creates the EMTDC model with a total length of 100 kM transmission lines by the use of distributed parameter line model, as shown in Fig. 5.

Line parameters:

$$r_1 = 0.02063\Omega / km\,;\, x_1 = 0.2810\Omega / km$$

$$C_1 = 4.0008\times10^{-6}\Omega / km\,;\, r_0 = 0.1626\Omega / km$$

$$l_0 = 1.1129\Omega / km\,;\, C_0 = 2.0742\times10^{-6}\Omega / km$$

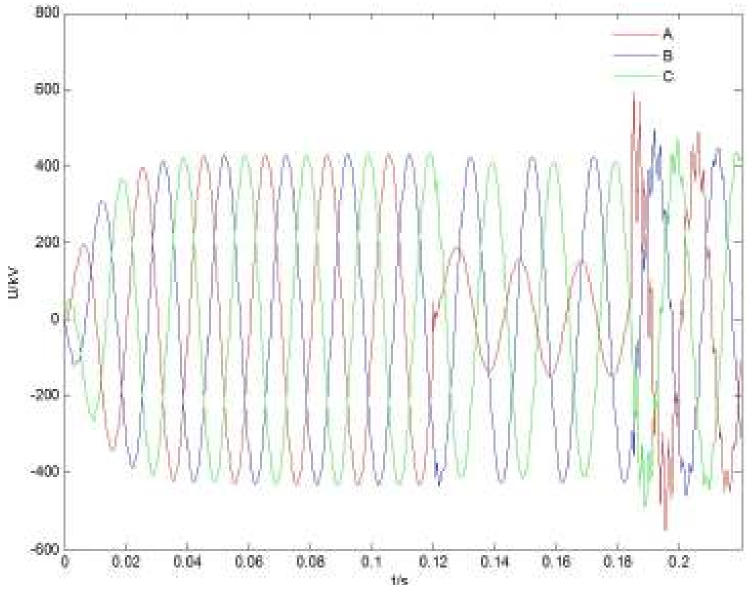

Fig. 6: Three-phase voltage of M side

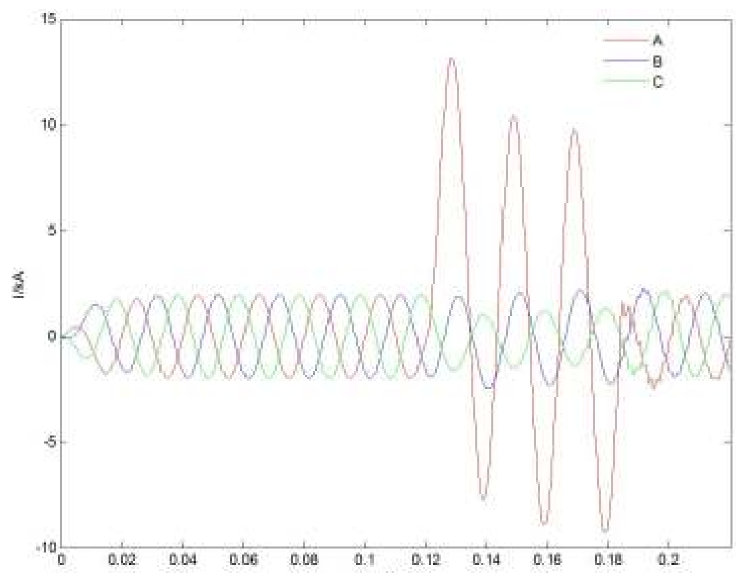

Fig. 7: Three-phase current of M side

System parameters of side M:

$$E_M = 1.05 p.u.\angle 0^0 ; R_{M1} = 1.0515\Omega ; L_{M1} = 0.13743H ;$$
$$R_{M0} = 0.6\Omega ; L_{M0} = 0.0926H$$

System parameters of side N:

$$E_N = 1.00 p.u.\angle -30^0 ; R_{N1} = 26\Omega ; L_{N1} = 0.14298H ;$$
$$R_{N0} = 20\Omega ; L_{N0} = 0.11927H$$

Sampling frequency is set to 16 kHz. It uses the differential full-wave Fourier algorithm for filtering. The simulation time is set to 0.22 sec and the ground fault occurs at 0.12 sec and it ends at 0.18 sec. PSCAD/EMTDC simulates the failure model, MATLAB processes the data. Figure 6 and 7 shows the voltage and current maps when a phase ground fault occurs at the point of 10 kM from M-terminal with grounding resistance is 10. And Fig. 8 shows the distribution diagram of function F (*l*).

It can be seen from the simulation results that when l is taken 0.1010, $F(L) = |Z_{M1} - Z_{M2}| + |Z_{M2} - Z_{M3}| + |Z_{M3} - Z_{M1}|$) is the minimum. Calculated distance is 10.10 kM, error distance is 0.10 kM, reached a distance requirements. In this study, different fault types transition resistances are simulated and analyzed by the tables followed.

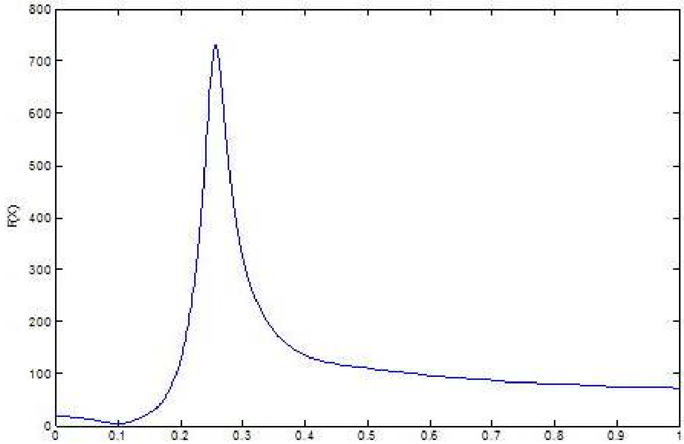

Fig. 8: *F* (*l*) distribution diagram

Table 1: Impacts of grounding resistance and fault location on the results of AG

	Failure distance/km							
	10		40		60		90	
Transition resistance/Ω	Measuring distance/km	Measuring error/km	Measuring distance/km	Measuring error/km	Measuring distance/km	Measuring error/km	Measuring distance/km	Measuring error/km
0	10.35	0.35	40.65	0.65	60.55	0.55	90.95	0.95
10	10.10	0.10	40.00	0.00	59.80	0.20	90.25	0.25
50	9.25	0.75	39.30	0.70	59.85	0.15	90.65	0.65
80	9.35	0.65	39.15	0.85	59.45	0.55	90.80	0.80
100	10.10	0.10	39.20	0.20	59.45	0.55	90.70	0.70

Table 2: Impacts of grounding resistance and fault location on the results of BCG

	Failure distance/km							
	10		40		60		90	
Transition resistance/Ω	Measuring distance/km	Measuring error/km	Measuring distance/km	Measuring error/km	Measuring distance/km	Measuring error/km	Measuring distance/km	Measuring error/km
0	10.35	0.35	40.75	0.75	60.40	0.20	90.55	0.55
10	10.60	0.60	39.25	0.75	60.15	0.15	90.05	0.05
50	10.20	0.20	40.15	0.15	59.80	0.20	89.75	0.25
80	9.55	0.45	39.80	0.20	60.30	0.30	90.15	0.15
100	10.55	0.55	39.90	0.10	59.75	0.75	89.55	0.45

Table 3: Impacts of grounding resistance and fault location on the results of ABC

	Failure distance/km							
	10		40		60		90	
Transition resistance/Ω	Measuring distance/km	Measuring error/km	Measuring distance/km	Measuring error/km	Measuring distance/km	Measuring error/km	Measuring distance/km	Measuring error/km
0	10.60	0.60	40.35	0.35	60.70	0.70	90.70	0.70
10	9.95	0.05	40.45	0.45	59.35	0.65	90.30	0.30
50	10.35	0.35	40.70	0.70	60.10	0.10	90.65	0.65
80	10.40	0.40	40.00	0.00	59.35	0.65	90.20	0.20
100	10.25	0.25	39.90	0.10	60.05	0.05	89.45	0.55

Table 4: Impacts of the length of transmission line on the results

	Failure distance/km							
	10		40		60		90	
Line length/km	Measuring distance/km	Measuring error/km	Measuring distance/km	Measuring error/km	Measuring distance/km	Measuring error/km	Measuring distance/km	Measuring error/km
50	10.15	0.15	39.95	0.05	60.00	0.00	90.10	0.10
100	10.10	0.10	40.00	0.00	59.80	0.20	90.25	0.25
150	10.25	0.25	39.35	0.65	59.80	0.20	89.55	0.45
200	9.20	0.80	40.60	0.60	60.95	0.95	90.80	0.80
225	10.85	0.85	42.15	2.15	58.95	1.05	89.35	0.65
250	20.90	10.90	55.35	15.35	51.25	8.75	108.90	18.90

It can be seen from Table 1 to 3 that the algorithm is largely unaffected by the fault location, fault type and transition resistance size. And it can still get a more accurate measurement result in the high-impedance grounding. It can be seen in Table 4 that it may achieve a better effect when the transmission distance is less than 200 km. When the length of transmission line is more than 200 km, the error is more than 1 km, exceeding the allowable range of engineering.

DISCUSSION

It is can be seen that the ranging accuracy of this algorithm meets actual project's needs. There is the analysis for the factors affecting the accuracy:

Transmission line length: From the results of the simulation, when the transmission line length exceeds 200 km, error exceeding 1 km and it does not meet the practical engineering requirement. It is because the algorithm ignores the distributed capacitance in the circuit when it equivalents the transmission line to series line which is consisting of self impedance and coupling impedance, when the line is not long, the distributed capacitance in the whole line may be ignored, the error does not exceed 1 km. But when the transmission distance is too long, distributed capacitance is large, distributed capacitive current time in the proportion of the entire circuit increases, the error will be increased, which cannot meet the project needs.

Filtering effect: A system asymmetrical failure occurs, it will generate a lot of high harmonics and decaying DC component, if filtering is not very good, it will have a huge impact on measuring electrical quantities and result in reduced range accuracy. Filtering effect will directly affect the size of measuring error. This study uses a differential full-wave Fourier algorithm and differential filtering and FIR low-pass filtering may also be used.

Hardware requirements and line conditions: Since the algorithm is based on GPS synchronous sampling, the hardware conditions are high, but the actual collection samples at both ends, generally there will be time errors, which will affect the ranging results, bringing the error.

CONCLUSION

A large number of simulation results show that this algorithm is not subject to transition resistance, system operating mode, fault type and fault distance influence. In the high-impedance grounding condition, it may still get accurate results. There is a good effect for the distance transmission line which is not too long and it has a high application prospect.

REFERENCES

Guo, Y., M. Kezunovic and D. Chen, 2003. Simplified algorithms for removal of the effect of exponentially decaying DC-offset on the Fourier algorithm. IEEE T. Power Deliver., 18(3): 711-717.

Huang, K. and L. Sun, 2003. A compact algorithm for filtering decaying DC component in relay protection Fourier algorithm. Power Syst. Automat., 27(4): 50-52.

Huang, F., M. Chen and H. Zhen, 2009. Improved difference FFT algorithms for fault location. Power Syst. Protect. Control, 37(11): 62-65.

Liang, J., C. Ma and Z. Yun, 2004. A fault location algorithm for high voltage overhead power transmission line based on line parameter estimation. Power Syst. Technol., 28(4): 60-63.

Qi, X., M. Ding and Y. Wen, 2005. An improved short data window full wave Fourier algorithm for completely filtering decaying DC component. Power Syst. Protect. Control, 33(17): 14-16

Suonan, J., Y. Zhang, J. Qi and Z. Jiao, 2006. Time domain fault location based on transmission line parameter identification using two terminals data. Power Syst. Technol., 30(8): 65-70.

Yu, S. and J. Gu, 2001. Removal of decaying DC in current and voltage signals using a modified Fourier filter algorithm. IEEE T. Power Deliver., 16(3): 372-379.